Plasma Research Express

RECEIVED
3 March 2020

REVISED
8 April 2020

ACCEPTED FOR PUBLICATION
27 May 2020

PUBLISHED
3 June 2020

TUTORIAL

Recent theory of traveling-wave tubes: a tutorial-review

Patrick Wong[1], **Peng Zhang**[1] **and John Luginsland**[2]

[1] Department of Electrical and Computer Engineering, Michigan State University, East Lansing, MI 48824, United States of America
[2] Confluent Sciences, LLC, Albuquerque, NM 87111, United States of America

E-mail: wongpat3@egr.msu.edu

Keywords: traveling-wave tubes, theory, traveling-wave amplifiers, electron beams, beam-circuit interaction, electromagnetic waves, space charge

Abstract

The traveling-wave tube (TWT), also known as the traveling-wave amplifier (TWA) or traveling-wave tube amplifier (TWTA), is a widely used amplifier in satellite communications and radar. An electromagnetic signal is inputted on one end of the device and is amplified over a distance until it is extracted downstream at the output. The physics behind this spatial amplification of an electromagnetic wave is predicated on the interaction of a linear DC electron beam with the surrounding circuit structure. Pierce, known as the 'father of communications satellites,' was the first to formulate the theory for this beam-circuit interaction, the basis of which has since been used to model other vacuum electronic devices such as free-electron lasers, gyrotrons, and Smith-Purcell radiators, just to name a few. In this paper, the traditional Pierce theory will first be briefly *reviewed*; the classic Pierce theory will then be extended in several directions: harmonic generation and the effect of high beam current on both the beam mode and circuit mode as well as 'discrete effects', giving a brief *tutorial* of recent theories of TWTs.

Introduction

Throughout the history of commercial and defense applications involving electromagnetics, there has always been a high demand for microwave and millimeter wave amplifiers that offer *both* high power output *and* wide bandwidth. One candidate that may fulfill these stringent requirements is the traveling-wave tube (TWT), also known as the traveling-wave amplifier (TWA) or traveling-wave tube amplifier (TWTA). This device is widely used in satellite communications and radar applications.

It turns out that a viable method of amplifying a given electromagnetic wave is by passing this signal through a periodic structure and co-propagating it with a linear DC electron beam. To reduce complexities, this beam-circuit interaction takes place in vacuum. In such a set-up, the traveling wave gains energy at the expense of the kinetic energy of the electron beam. This continuous interaction and subsequent amplification of the electromagnetic wave happens over a distance (the length of the interaction region of the TWT) until the amplified wave is extracted at the output.

Before the invention of the TWT, the klystron amplifier (1935) was one of the first microwave amplifiers used [1–4]. This device though had several limitations. The most notable one is that the klystron had narrow bandwidth, as amplification is restricted to the resonant frequencies of the klystron cavities. The idea then came about to couple the individual cavities of a multi-cavity klystron to a common transmission line so that there may be a continuous in-phase interaction between beam and circuit [3, 4]. This eventually led to the development of the traveling-wave tube amplifier. Figure 1 shows the evolution of the klystron to the traveling-wave tube.

Rudolph Kompfner of England, interestingly an architect by profession, was the first to propose the idea of a traveling-wave tube. He and Nils Lindenblad of the United States used a metallic helix as the circuit structure for propagating the signal in phase with the centered pencil electron beam in vacuum and are credited with being the first to create the TWT as it is known today [5, 6]. Prior to this, Haeff proposed a similar idea but had the electron beam on the outside of the circuit, leading to poorer efficiency [7]. Kompfner's invention of the TWT then aroused the intense interest of John R Pierce who then laid the foundation of the TWT theory and was later

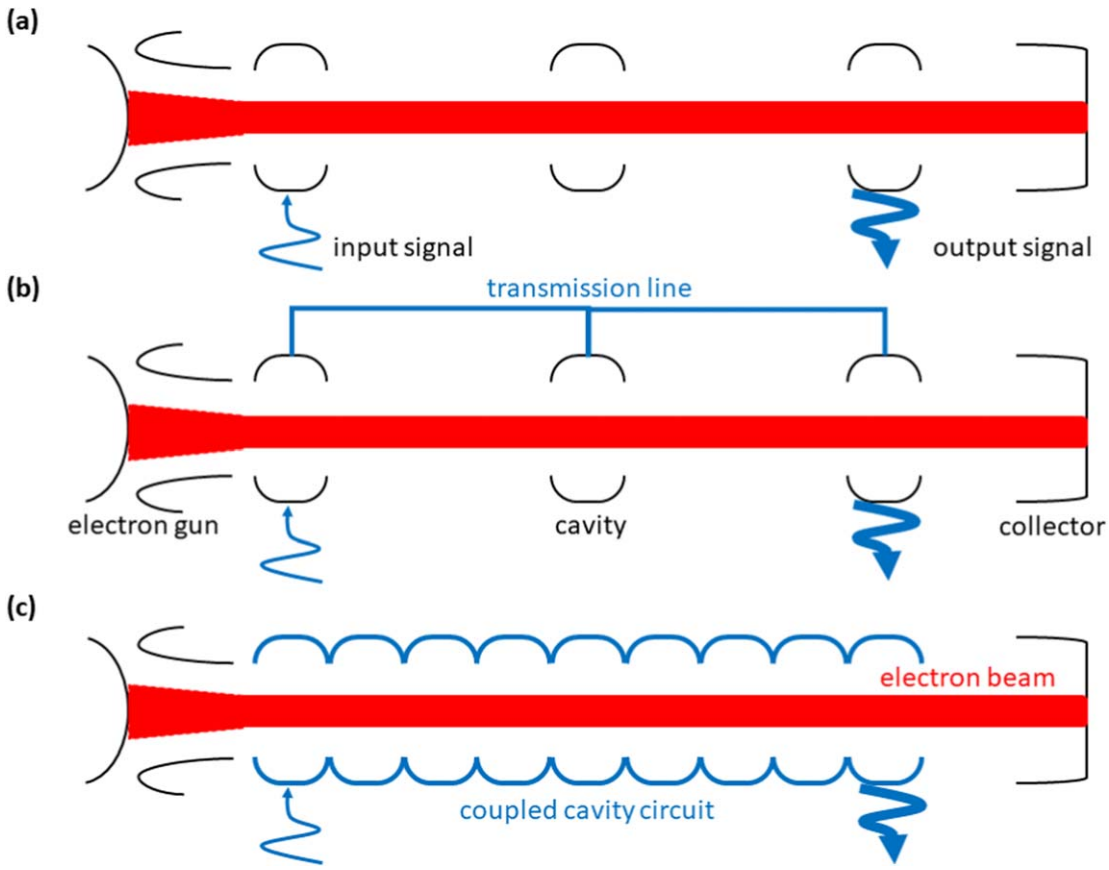

Figure 1. Schematic diagram showing the evolution of a multi-cavity klystron (a) to a traveling-wave tube amplifier (c). (b) shows the multi-cavity klystron with its cavities coupled to a common transmission line.

known as the 'father of communications satellites' [8]. A schematic diagram of a modern TWT is shown in figure 2.

As can be seen in figure 2, an actual TWT is a complex device, consisting of components (left: cathode, electron gun, etc) that create and form the electron beam, the beam-circuit interaction region (middle: helix, electron beam, etc), and components (right: collector) that collect the 'spent' beam. Each of these topics in and of themselves constitute a library of study. In this paper, the focus will be restricted to the physics in the beam-circuit interaction region within the helix (figure 2). In particular, the standard beam-circuit mode coupling theory of Pierce will be examined. Using the Pierce theory as a basis, we will then extend it to describe effects originally neglected by Pierce: harmonic generation and the effects of high beam current on the circuit as well as connecting the continuous wave picture of Pierce to a discrete circuit formulation.

To begin, it must be emphasized that the operation of a TWT, or virtually any beam-driven microwave source, is predicated on the interaction of an electron beam in vacuum with an in-phase, co-propagating electromagnetic wave on a circuit structure. As such, it is instructive to analyze each of these two components: beam and circuit separately and then describe their interaction, as was also done by Pierce [10]. This method of analysis and mode coupling is not restricted to TWTs, rather, the techniques presented here are quite general and applicable to all beam-circuit interactions between charged particles and electromagnetic radiation.

The electron beam

As can be seen in figure 2, the electron beam is formed outside of the beam-circuit interaction region. Electrons are boiled off from a thermionic cathode (thermionic emission) or emitted from a material using strong electric fields (field emission). In either scenario, a voltage is externally applied to the cathode and this is essentially the kinetic energy of the beam entering the interaction region. We will denote the kinetic energy of this beam by voltage V_b, corresponding to a DC beam velocity v_0. Invoking conservation of energy in the non-relativistic regime,

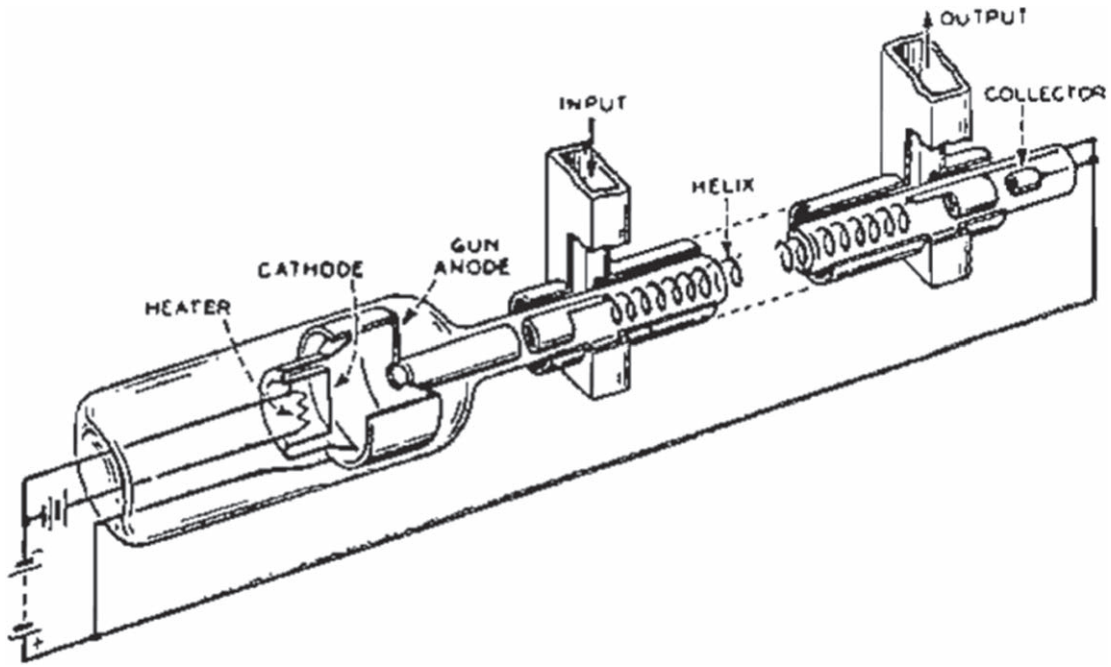

Figure 2. Schematic diagram of a traveling-wave tube amplifier. There are many components to a TWTA. In this paper, we will concentrate only on the middle section, the helix, of the above figure: the beam-circuit interaction region. The slow-wave circuit shown here is a helix (with support rods). Image from [9]. This diagram of helix TWT has been obtained by the author(s) from the Wikipedia website, where it is stated to have been released into the public domain. It is included within this article on that basis.

$$v_0 = \sqrt{\frac{2eV_b}{m_e}}. \tag{1}$$

For simplicity, it is assumed that there are no temperature effects on the beam so that the beam is 'cold' or mono-energetic (introducing temperature effects will be slightly more complicated but will essentially introduce a spread in electron velocities centered around a mean value). We further assume that the DC beam motion is one-dimensional, i.e., we implicitly assume that there is an infinite axial magnetic field confining the beam. In reality, this is provided by an external solenoid or periodic permanent magnets.

The current density of the beam is then defined as: $J = \rho v$, where ρ is the charge (electron with charge $-e$ and mass m_e) density of the beam. This current density is related to the beam current, which is externally adjustable, by $I_0 = JS = \rho_0 v_0 S$, where S is the cross-section of the beam. Thus,

$$\rho_0 = \frac{I_0}{v_0 S}. \tag{2}$$

The two externally adjustable parameters of the beam: the DC beam voltage V_b and the DC beam current I_0 control the unperturbed electron beam velocity v_0 and the electron charge density ρ_0, respectively. In the absence of any perturbation, the electron beam travels through vacuum in the axial direction with these unperturbed properties.

An input signal of frequency ω would induce a density perturbation on the beam, ρ_1, whose characteristic propagation constant on the beam is $\beta_e = \omega/v_0$. That is, the wave-like density perturbation on the beam is carried along the beam with the beam's unperturbed velocity v_0. The simple relation, $\omega = \beta v_0$, is often known as the beam mode, where β is the wavenumber or propagation constant (usually designated as k in the plasma physics literature). For a fixed ω (and DC beam velocity v_0), $\beta = \beta_e$, the 'electronic' wavenumber defined above. This beam mode is the dispersion relation for a one-dimensional linear electron beam with drift velocity v_0, relating the frequency of a mode of propagation to the corresponding propagation constant. Furthermore, a velocity perturbation v_1, a current perturbation I_1, and an electric field (or electric potential) perturbation E_1 would also be introduced to the beam by the signal. With this understanding, and using a simple model of the beam as a non-neutral plasma with the fluid model, the governing equations for the velocity and density perturbations on the beam can be written down, relating these quantities to the perturbed electric field and beam current:

$$\left(\frac{\partial}{\partial t} + v\frac{\partial}{\partial z}\right)v = -\frac{e}{m_e}E, \tag{1'}$$

$$\frac{\partial \rho}{\partial t} + \frac{\partial J}{\partial z} = 0, \tag{2'}$$

where the dependent variables $\{v,\ E,\ \rho,\ J\} = \{v_0,\ E_0,\ \rho_0,\ J_0\} + \{\widetilde{v_1},\ \widetilde{E_1},\ \widetilde{\rho_1},\ \widetilde{J_1}\}\, e^{j\omega t - j\beta z}$ consists of the unperturbed DC part (subscript '0') and a linear wave-like AC perturbation (subscript '1') due to the signal at frequency ω[3]. Substituting this linear expansion into equations (1′) and (2′) and taking advantage of the fact that the unperturbed quantities are constant in space and time, one can derive the 'linearized' force law and continuity equation for the beam electrons respectively:

$$\left(\frac{\partial}{\partial t} + v_0\frac{\partial}{\partial z}\right)v_1 = -\frac{e}{m_e}E_1 \rightarrow j(\omega - \beta v_0)\widetilde{v_1} = -\frac{e}{m_e}\widetilde{E_1}, \tag{1'a}$$

$$\frac{\partial \rho_1}{\partial t} + \frac{\partial J_1}{\partial z} = 0 \rightarrow j(\omega - \beta v_0)\widetilde{\rho_1} = j\beta\rho_0\widetilde{v_1}, \tag{2'a}$$

remembering that the current density is the product of the charge density ρ and the velocity v. Here, the axial electric field E_1 is a superposition of a component due to the electromagnetic signal (circuit wave) E_C and a component due to the space charge of the beam E_{SC}. The space-charge term will modify the beam mode, but accurate modeling of this term remains elusive. We shall return to this point later on (see section 'Beyond Pierce'). The governing equations, as they are now, are not closed (3 variables: $\{v,\ E,\ \rho\}$ with 2 equations). There must be at least one more independent equation: this comes in the form of the so-called slow-wave circuit equation that describes how the electromagnetic wave reacts to the electron beam. This is described in the next section.

The electromagnetic circuit

In vacuum, an electromagnetic signal, a transverse electric and magnetic (TEM) wave, propagates at the speed of light, c. However, for there to be appreciable gain for the input signal, the condition of synchronism between the wave and electrons in the beam must be satisfied. That is, $v_0 \approx v_{ph}$, where v_{ph} is the component of the phase velocity of the wave that co-propagates with the beam. This synchronism condition is required for the beam's kinetic energy to be effectively transferred to the wave energy of the electromagnetic signal. Since the speed of the electrons cannot exceed c, one must slow down the phase velocity of the wave in the direction of beam propagation so that this condition of synchronism is achieved. This is realized through the use of a slow-wave structure (SWS). A good SWS is designed so that the signal has the axial projection of its phase velocity about equal to the beam velocity over a wide range of frequencies for broad-band amplification. A metallic helix wire has such a property and thus is one reason why it is widely used in the industry and why we will analyze it here.

There are of course other SWS designs for different purposes. A listing and description of some of these SWS designs can be found in [11]. Traditionally speaking, all of the structures are metallic, but much effort has, in recent years, been placed in studying metamaterial SWS's [12, 13]. These have very different dispersion characteristics than their metallic counterparts leading to different gain properties. However, their beam-circuit interaction may still be captured by the mode-coupling theory of Pierce (in the small-signal regime); the physics and mathematics of the beam and circuit coupling remains the same. Different beam configurations (e.g. pencil beam versus sheet beam versus annular beam) will also play a role in the gain characteristics of the tube (see [11a] for a comparison between pencil and annular beams and [11b] for a discussion comparing sheet beams, an 'unwrap' of annular beams, to pencil beams; [14] talks about the plasma frequency reduction factor for different beam configurations, a topic we will come back to soon). Still to this date though, the helix SWS coupled with a pencil electron beam remains the 'go-to' for high power microwave amplification because of its wide bandwidth and ease of construction.

The reason why a helix TWT may offer a wide bandwidth is qualitatively illustrated in figure 3.

Figure 3(a) shows a very thin metallic wire over a perfectly conducting plane. This idealized system admits a TEM wave that propagates along the wire at the speed of light, regardless of the frequency. Moreover, since the RF electric and RF magnetic fields of this TEM mode decay like $1/r$ from the wire, for a thin wire (r being the distance away from wire), the electromagnetic power carried along this thin wire will then be concentrated in the immediate vicinity of the thin wire. It is then easy to understand the figure shown in figure 3(b): a thin helix inside a conducting cylindrical waveguide is able to transport electromagnetic energy in the vicinity of the wire at the light speed along the helix, for a very wide range of frequencies, i.e., wide bandwidth. The phase speed of this TEM mode along the z-axis is greatly reduced from c if the helix is tightly wound. From figure 3(b), the incremental distance (ds) along the helix of diameter d and pitch p is $ds = \sqrt{\left(\frac{d}{2}d\theta\right)^2 + (dz)^2} = dz\sqrt{1 + \left(\frac{d}{2}\frac{d\theta}{dz}\right)^2} = dz\sqrt{1 + \left(\frac{d}{2}\frac{2\pi}{p}\right)^2}$. Since $\frac{ds}{dt} = c$, for the TEM wave propagating along the helix, the phase speed of this local TEM wave projected along the z-axis is, $\frac{dz}{dt} = \left(\frac{ds}{dt}\right)\frac{1}{\sqrt{1 + (\pi d/p)^2}} = c\frac{p}{\sqrt{p^2 + (\pi d)^2}} \equiv v_{ph}$. Note that v_{ph} is independent of frequency in this approximation. Thus, the

[3] What happens if we keep more terms in the expansion? See the section, 'Beyond Pierce' below.

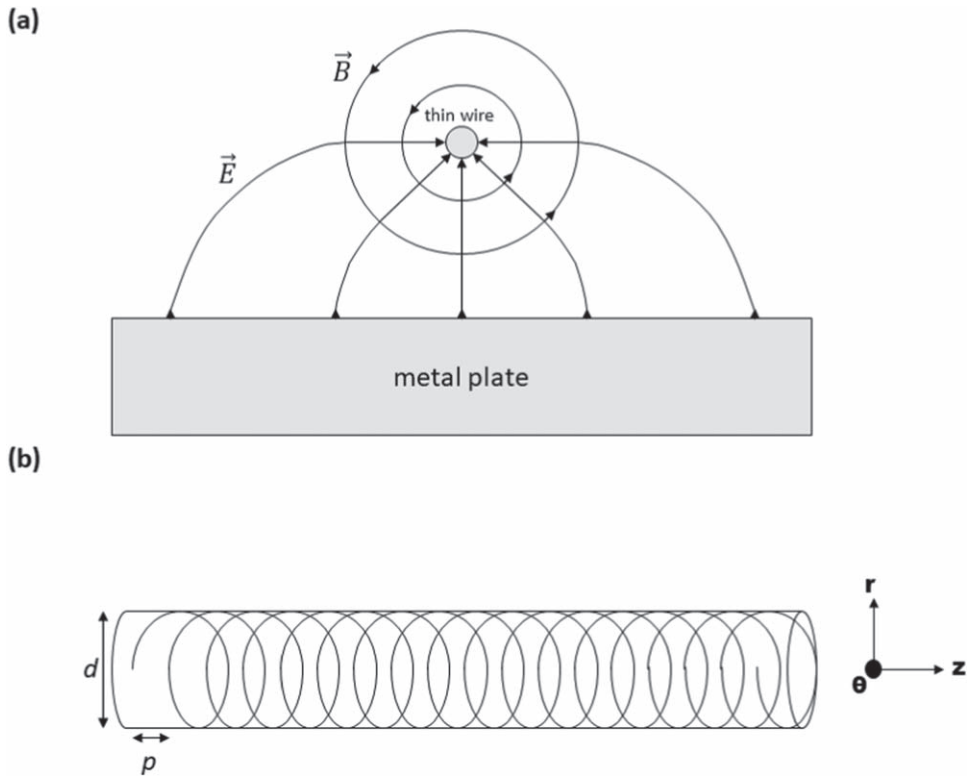

Figure 3. (a) Depiction of the TEM fields of a thin wire over a perfectly conducting metal plate. (b) The formation of a helix TWT from 'wrapping' the set-up in (a).

synchronism condition for beam-circuit interactions, $v_0 \approx v_{ph}$, may be maintained over a wide frequency band. Since this phase velocity is independent of the frequency of the injected signal ω, multiple octave bandwidths for the helix TWT are a reality. This fact prompted our investigation of harmonic generation.

Because we are essentially dealing with the propagation of electromagnetic waves in some media, it should be expected that the governing equation for the electric field on the circuit will be the Telegrapher's Equations and hence the Wave Equation (or Helmholtz Equation with a wavenumber along the direction of beam propagation, $\beta_{ph} \equiv \omega/v_{ph}$) with some modification due to the presence of the beam. This is indeed the case:

$$\frac{d^2E_C}{dz^2} + \Gamma_0^2 E_C = j\Gamma_0\beta_{ph}^2 K J_1 S \tag{3}$$

where E_C is the circuit electric field, Γ_0 is the effective propagation constant of this circuit wave ($=\beta_{ph}$ with an imaginary part to account for attenuation in the circuit), and K is known as the interaction impedance (essentially a pure geometrical quantity that is a proportionality constant between the voltage and current of the 'cold' no beam system). Assuming time and spatial harmonic fields, equation (3) may be written as:

$$\widetilde{E_C} = \frac{j\Gamma_0\beta_{ph}^2 K}{\Gamma_0^2 - \beta^2}\widetilde{J_1}S, \tag{3a}$$

which gives the circuit electric field $\widetilde{E_C}$ excited by the beam's AC current $\widetilde{J_1}$ at frequency ω. Note that if there is no electron beam, $\widetilde{J_1} = 0$, there will be a non-zero circuit electric field $\widetilde{E_C}$ only if $\beta = \Gamma_0$, which is the vacuum circuit mode dispersion relation (compare this to the beam mode dispersion relation considered above), and this circuit electric field $\widetilde{E_C}$ is then simply the vacuum mode solution. In other words, if $\beta = \Gamma_0$, any finite AC current on the beam will yield an infinite response on the circuit electric field $\widetilde{E_C}$, a well-known fact for synchronous excitation, as clearly shown in equation (3*a*). It should be noted that this analysis of the circuit, following Pierce [1–4, 10], deals only with the fundamental passband and its interaction with the beam. Because of this, Pierce's theory is also used for the interaction between a single space harmonic of the circuit and the fundamental mode of the beam to assess the strength of interaction at that space harmonic. In general though, there are an infinity of passbands and space harmonics of the circuit mode *and* the beam mode, as we will soon see.

To illustrate what the different modes of propagation look like for a TWT, a sample Brillouin or cold-tube dispersion diagram (ω versus β plot, obtained from $\beta = \Gamma_0$, the expression for which is given in [15]) is shown in figure 4 for the 'tape' helix (a model of the helix with finite width but infinitesimal thickness in the radial direction). In this example, no cold-tube circuit loss is assumed ($\mathrm{Im}(\Gamma_0) = 0$, there is no attenuation in the

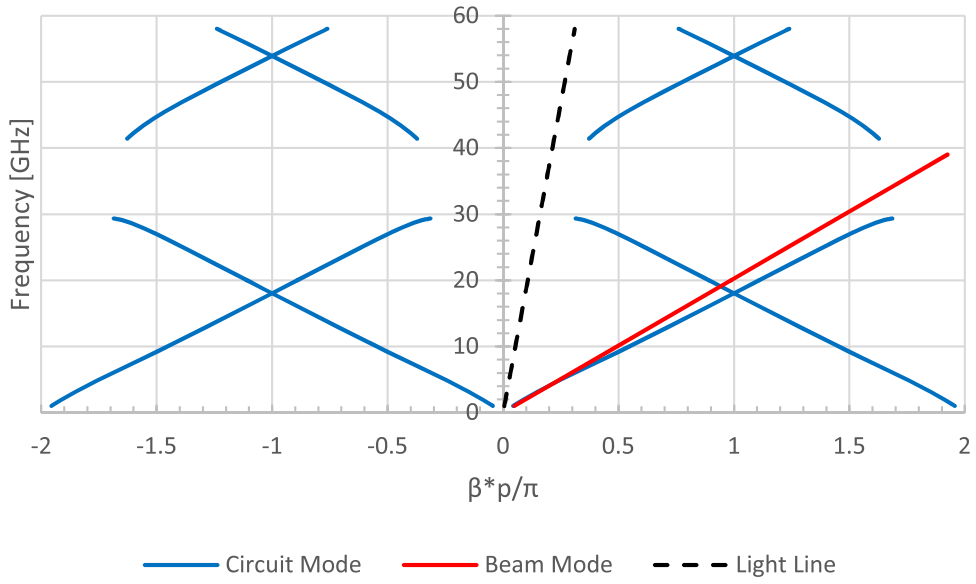

Figure 4. Dispersion diagram for a tape helix showing several circuit modes ($\beta = \Gamma_0$, blue) and the beam mode ($\beta = \frac{\omega}{v_0}$, red). Also included in the Figure is the light line ($\beta = \frac{\omega}{c}$, black, dashed).

circuit). This tape helix has a period p and has multiple passbands (two shown in figure 4 in blue). In between these passbands are stopbands where no signal can be supported by the circuit. One should note the periodic nature of each passband corresponding to the space harmonics n (starting with $n = 0$ in the middle and moving outwards; the segments with positive slope correspond to the positive space harmonics and the segments with negative slope correspond to the negative space harmonics). The propagation constant, β_n, of the nth spatial harmonic is:

$$\beta_n = \beta_0 + \frac{2\pi n}{p}, \quad n = 0, \pm 1, \pm 2, \ldots, \tag{4}$$

β_0 (or just β in the literature) is called the fundamental, and β_n ($n \neq 0$) is called the nth space harmonic.

The beam mode $\omega = \beta v_0$ (as discussed before) is also shown in figure 4 in red. As can be seen, the synchronism condition ($v_0 \approx v_{ph}$) between the beam mode and the circuit mode is satisfied for a wide range of frequencies. This is what gives the tape helix its characteristic wide bandwidth.

Note that the point of operation for a TWT is where the beam mode (red) intersects the circuit mode (blue) on the fundamental branch; as discussed before, this is where synchronism between beam and circuit is the strongest. However, astute observers of figure 4 will note that the beam mode intersects the circuit mode at more than one point, on the other branches of which there are an infinity of them (not shown here). These 'residual' modes are important and will be discussed later along with the mirror problem of the intersection of the circuit mode with the infinity of beam modes besides the fundamental (c.f. equation (4)). For now, we just want to point out that the type of intersection between circuit and beam matters: for amplification (generally what we desire for a TWT), the circuit mode has a positive slope. If the beam mode were to intersect the part of the circuit mode with a negative slope (e.g. the $n = -1$ branch), backward wave oscillations will occur as the group velocity of the circuit wave is in the opposing direction to the beam motion [16]. At the crossing between the forward and backward circuit mode branches, the 'band edge' where there is zero group velocity and the two waves are tightly coupled, an instability known as the 'absolute instability' can occur [17–19]. To be specific, this possible 'absolute instability' is the 'π-point absolute instability' (as it occurs for the phase advance of $\beta p = \pi$), which is different from the 'absolute instability' that can occur from the beam interaction with the backward wave. In either case, near the 'band edge' or not, the 'absolute instability' is the result of the beam interacting with a dispersive medium with internally provided feedback leading to oscillations in the tube [18]. Oscillations in a TWT occurring from deliberately exciting a backward wave or from the 'absolute instability' (or even from impedance mismatches at the ends of the circuit) are beyond the scope of this paper. We only note that they are dangerous to TWT operation.

What we have allured to but have neglected to discuss thus far is the space-charge electric field E_{SC} coming from the beam, with good reason. Space-charge calculations in general are notoriously difficult, and there is no general model that can capture this internal self-force of the beam. It turns out, see the section 'Beyond Pierce', that one model of space-charge effects is intimately tied to the higher-order passbands of the circuit and the

higher-order beam modes. This higher-order interaction was not initially captured by Pierce as his analysis was concerned with the interaction of the fundamental passband and beam mode only. It should be noted though that he did hypothesize the role of higher-order passbands of the circuit on space charge; for now, we will group space-charge effects under the term 'QC' or 'Q', following Pierce's original notation. Thus, accessing space-charge effects in TWTs boils down to finding an expression for 'Q', known as Pierce's AC space-charge parameter.

The Beam-Circuit Interaction and Pierce's theory of mode-coupling

Now that we have described the beam and circuit separately, how do they interact in such a way to produce amplification of the injected signal? When the beam enters the beam-circuit interaction region and feels the circuit wave, the electrons in the beam will respond to the sinusoidal nature of the electric field of the signal. Consequently, one can imagine that some electrons will be accelerated by the accelerating portion of the wave and some electrons will be decelerated by the decelerating portion of the wave. This leads to the formation of electron bunches in the electron beam. These bunches in turn cause the electric field in the circuit to increase by inducing more current in the circuit; electron motion inducing currents in external circuits can be attributed to the famous Shockley-Ramo Theorem [20]. The resulting amplitude increase in the electric field in the circuit causes more bunching in the beam. The physical mechanism is succinctly illustrated in Gilmour's book [1, 2].

From a wave mechanics picture, a pair of space-charge waves on the electron beam are created from the beam interacting with the circuit wave. These space-charge waves on the beam are analogous to longitudinal pressure waves in air consisting of compressions and rarefactions. In this case, we have the fast and slow space-charge waves that co-propagate on the electron beam with the circuit wave. The energy difference from the slowing-down of the electrons in the beam to the slow space-charge wave phase velocity is given to the circuit, causing amplification of the circuit wave. This beam-circuit interaction has proven to be effective: the growth of the input signal, at least in the small-signal regime, is exponential with distance along the tube [1, 2]. TWT power gain of 60 dB (1 million times) can be realized [21].

Eventually, as more bunching occurs, the space-charge forces of the beam will cause the electron bunches in the beam to de-bunch. Furthermore, other effects such as the slowing down of the beam as a whole due to the loss of energy to the circuit will limit TWT gain because the synchronism condition ($v_0 \approx v_{ph}$) is no longer satisfied [1, 2, 4]. Phenomena such as saturation, wave-trapping of electrons, etc. constitute full non-linear operation of the TWT. These advanced topics are beyond the scope of this text. The linear or small-signal theory discussed here is important as it essentially feeds into the non-linear theory (the formulation of non-linear theory is predicated on the concepts introduced in the linear theory) and is stated to be able to accurately describe ~85% of the tube length [1, 2, 4]. Historically speaking, the linear theory was also the first comprehensive theory developed to describe the inner workings of the beam-circuit interaction. Because of this, we will focus mainly on the linear theory and its quasi-linear extension when we consider harmonic generation.

As stated before, the classical theory of beam-structure interactions in a TWT was developed by Pierce [10], whose treatment also provided the foundations for the understanding and design of a wide range of contemporary sources such as free-electron lasers [4, 22–24], Smith-Purcell radiators [4, 23–26], gyrotron amplifiers [4, 26–30], metamaterials TWTs [12, 13, 31], and NonLinear Transmission Line (NLTL) based sources [32]. We will present the standard Pierce theory and further develop it to indicate other novel effects not previously considered by Pierce. Pierce described the energy transfer mechanism in terms of the interaction between the space-charge waves on the electron beam and the electromagnetic mode supported by the electromagnetic circuit. Amplification of a signal of frequency ω is described by the complex wavenumber β that is a solution of what is known as the Pierce dispersion relation, which, in its most basic form [1, 3, 4, 10, 13, 22–24, 26–30], is a third-degree polynomial for $\beta(\omega)$. This dispersion relation describes the coupling between the beam mode and the circuit mode [33, 34]. It has been used in the validation of non-linear, large-signal numerical codes in the small-signal regime.

An interesting side note is that unlike most topics, such as plasma physics and electromagnetic wave theory, here we consider the propagation constant as a function of the frequency. That is, one is generally given a frequency (the frequency of the input signal to be amplified) and is tasked with finding the corresponding propagation constant, which is in general complex. The imaginary part corresponds to either the growth (amplification) or decay (attenuation) of the wave in the system.

We are now in a position to self-consistently solve the governing equations for the beam (equations (1), (2)) and circuit (equation (3)) to yield solutions describing the evolution of both, as a coupled system. With some manipulation, the three equations can be combined to yield:

$$[(\beta - \beta_e)^2 - \beta_e^2 4QC^3][\beta^2 - \Gamma_0^2] = -2\beta_e\beta_{ph}^2\Gamma_0 C^3, \tag{5}$$

which is known as Pierce's 4-wave dispersion relation. It is called as such because the solution of this relatively simple fourth-order polynomial for the propagation constant β given the frequency of the input signal ω yields four roots, with each root corresponding to a permitted mode of propagation or wave. The equation itself has a satisfying interpretation: the first square bracket on the LHS represents the beam mode (2 forward propagating space-charge waves), the second bracket represents the cold-tube circuit mode (1 forward and 1 backward propagating circuit waves), and the RHS represents the coupling of the two. The quantity $C^3 \equiv \frac{KI_0}{4V_b}$ on the RHS of equation (5) (also appearing in the beam mode on the LHS) is known as Pierce's gain parameter or also as Pierce's coupling constant. This dimensionless parameter is called as such because it gives a measure of the gain of the TWT while also giving a measure of the degree of coupling between the beam and circuit.

To simplify matters (this was back in the day when solving quartic polynomials was a chore!), a common approximation is to assume that C is small and to neglect the backward circuit wave, as it is primarily the forward waves that contribute to the gain of a TWT downstream. Doing so and using the notation of Pierce, the so-called 3-wave dispersion relation reads:

$$(\delta^2 + 4QC)(\delta + jb + d) = -j, \tag{6}$$

where

$$\delta \equiv \frac{\beta - \beta_e}{\beta_e jC}, \tag{7}$$

$$b \equiv \frac{v_0 - v_{ph}}{Cv_{ph}}, \tag{8}$$

$$d \equiv \frac{\mathrm{Im}(\Gamma_0)}{\beta_e C}. \tag{9}$$

For comparison purposes (c.f. equation (5') below), Pierce's 3-wave dispersion relation for β reads:

$$[(\beta - \beta_e)^2 - \beta_e^2 4QC^3][\beta - \beta_{ph}] = -\beta_e^3 C^3. \tag{6a}$$

One would solve equation (6) for the incremental propagation constant δ (or equation (6*a*) to find the real physical parameter β) knowing the detune parameter b, circuit loss parameter d, gain parameter C, and space-charge parameter Q. Collectively, the dimensionless parameters $\{C, Q, b, d\}$ are known as the Pierce parameters and they completely characterize a given TWT set-up. These parameters are ubiquitous in the tube literature and industry; even the more complete large-signal analysis uses these parameters as input. The values of these parameters with the exception of the notorious space-charge parameter Q may be determined apriori from just knowing the basic properties of the beam and cold circuit structure. Typical numerical values are:
$\beta \sim \beta_e \sim \beta_{ph} \sim O(1)$, $C \sim O(10^{-3} - 10^{-1})$, $Q \sim O(1 - 10)$, and $d \sim O(1)$.

It should be noted that reflection from the ends and waves near the band edges cannot be accounted for by Pierce's 3-wave theory. A classical look into Pierce's 4-wave theory and its reduction to the 3-wave theory is provided by Birdsall and Brewer [35]. The importance of the 4-wave description, and the effects of reflection on the TWT stability may be found in [36–38].

Beyond pierce

The above was a tour-de-force through electron beam dynamics and electromagnetic wave theory culminating in a simple yet powerful description of beam-circuit mode coupling and interaction in a TWT. One must remember that this type of analysis was done back in the early to mid-20th century. Many advancements in terms of modeling and mathematics and the advent of scientific supercomputing have taken analyses of such devices to new heights. Consequently, more complex and accurate descriptions on the inner workings of a TWT exist. Nevertheless, there is still a subtle charm to a simple theory. Not only can it give a 'back-of-the-envelope' assessment of a given problem but it can provide great physical insights into the nature of such interactions and processes. In this vein, we will now attempt to relax some of the assumptions of Pierce and extend his theory in a simple manner and draw further insights into the beam-circuit interaction. The topics covered here will be harmonic generation and space charge in TWTs as well as 'discrete cavity' effects, relating TWT analysis to klystron analysis. A brief synopsis of the first two topics are provided in the following paragraphs.

The classical Pierce theory was formulated for a single (fundamental) frequency, that of the input signal. However, in a TWT with an octave bandwidth or greater, in particular the widely used helix TWT, the second harmonic of the input signal may also be within the amplification band and thus may also be generated and amplified, with no input at this second harmonic frequency. An extension to the Pierce formulation that incorporates the generation of harmonics will be presented here. It is shown that the second harmonic arises

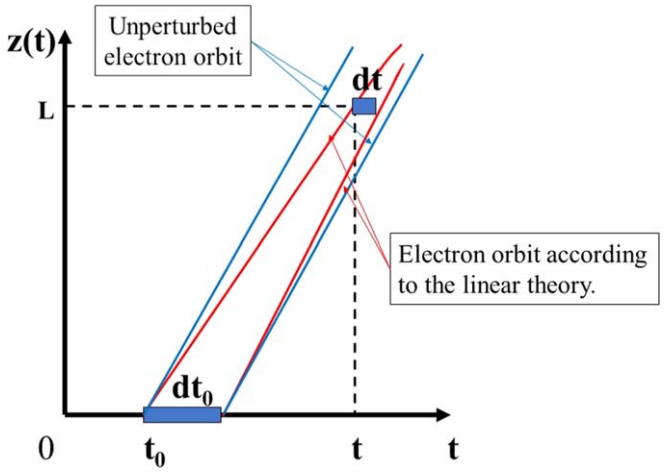

Figure 5. An (exaggerated) illustration of harmonic generation due to orbital crowding. Crowding in the linear orbits may lead to harmonic current generation, as shown in klystron theory [3] and TWT theory [43].

mostly from a newly discovered dynamic synchronous interaction instead of by the kinematic orbital crowding mechanism that is the most dominant harmonic generation mechanism in other microwave devices. The methodology provided here, which is a natural extension of Pierce's original theory, may be applicable not only to TWTs but to other high-power microwave sources.

In beam-circuit interactions, the space-charge effect of the beam is important at high beam currents. In Pierce's TWT theory, as stated before, this space-charge effect is modelled by the parameter which he called Q in the beam mode. A reliable determination of Q remains elusive for a realistic TWT. Previously, Wong *et al* [39] constructed the first *exact* small-signal theory for the beam-circuit interaction for the tape helix TWT, from which Q may be unambiguously determined. In the process of doing so, it was discovered that the circuit mode in Pierce's theory must also be modified at high beam current, an aspect overlooked in Pierce's original analysis. This circuit mode modification is quantified by an entirely new parameter called q, introduced for the first time in TWT theory. For the example using a realistic tape helix TWT, we find that the effect of q is equivalent to a modification of the circuit phase velocity by as much as two percent, which is a very significant effect. A brief summary of q will be provided here.

Harmonic generation in TWTs

The subject of harmonic generation in a TWT has traditionally been studied in the non-linear, large-signal regime. We will not delve into large-signal theory here as it is beyond the scope of this text. The theory itself is more complete as it can not only capture non-linear phenomena such as saturation, wave-trapping of beam electrons, etc. but can also recover the linear, small-signal regime. However, it is much more complicated than the relatively simple linear theory presented here thus far and simple insights, which we stress here, cannot be easily drawn. We will note here that large-signal TWT theory and also the study of harmonics of the input signal can be traced back to the classical paper by Nordsieck [40], who also provided the first analysis of TWT efficiency. References may be made to Tien *et al*, Rowe, Giarola, and Dionne [41] whose subsequent works relied heavily on Nordsieck's initial theory.

Taking a step back, it is well-known in klystrons that the dominant cause of harmonics of the input signal to be generated is due to linearized orbital motion from an input signal leading to orbital crowding, which leads to harmonic generation kinematically [3, 42] (see figure 5 below). In such scenarios, the extreme case of charge overtaking may also occur and contribute to harmonic generation. It was not until recently that such a theory on harmonic content in the beam current of a TWT was developed by Dong *et al* [43] in the small-signal regime. In that work, the linearized electron orbits might lead to a second harmonic AC current as high as 25% of the DC beam current, and this was favorably compared to the large-signal TWT code CHRISTINE [44].

A little after Dong *et al*'s paper, another source of harmonic content in a TWT was discovered: weak non-linearities in the electron orbits. It turns out, with respect to the RF power output, that this source of harmonic generation is much more important as it possesses the property of *synchronism between the beam and circuit in both space and time*, the underpinning concept behind the operation of TWTs. The effect of orbital crowding described in the preceding paragraph is negligible in comparison [45].

The main idea behind this alternative view on harmonic generation in TWTs stems from carrying out higher-order expansions of the governing equations for the beam [recall: Pierce's small-signal analysis is a linear theory; this is the answer to the above question posed in Footnote 1]. These minor corrections on the quantities of the beam corrects the linear quantities of Pierce [46] but also turn out to be the harmonics; basically, we regard the quantities of interest: the electric field (potential), beam density and velocity (current) to be represented by a Fourier series. This interpretation then is a quasi-linear theory.

The electromagnetic signal causes the electrons in the beam to bunch. To first order, these bunches are at the frequency of the signal itself, leading to Pierce's linear theory. The orbits of the beam electrons though are better represented at higher orders and thus contain more frequencies of the input signal. In response, the circuit picks up each of these frequencies individually (Maxwell's Equations are linear). The circuit then not only supports an amplifying signal at the fundamental (input) frequency but also a spectrum of harmonics of the original signal, all being spatially amplified. This of course can only happen if the spectrum of frequencies is within the bandwidth of the TWT: any frequency outside of the characteristic bandwidth will not be supported by the structure. The ubiquitous helix structure is one such circuit structure that can have octave bandwidth, as evidenced by figure 4 above.

Put another way, if we inspect the equation for the beam, equation (1′), and continue the expansion beyond order 1 (Pierce), we will find, for example for $n = 2$, the non-linear convective derivative in the force law, $v_1 \frac{\partial v_1}{\partial z}$, where $v_1 = v_{10} e^{j\omega_0 t - j\beta_0 z}$ is the *linearized* electron fluid velocity at the fundamental frequency, whose wavenumber $\beta_0 \approx \frac{\omega_0}{v_0}$ where v_0 is the DC beam velocity. This convective derivative, $v_1 \frac{\partial v_1}{\partial z}$, then contributes a "force" proportional to $v_{10}^2 e^{j2\omega_0 t - j2\beta_0 z}$ (analogous to the 'ponderomotive force' in the latter's derivation [47]). This 'force" is a traveling wave at the second harmonic frequency. It has a phase velocity also synchronized with the electron beam because $\frac{\omega}{\beta} = \frac{2\omega_0}{2\beta_0} = \frac{\omega_0}{\beta_0} \approx v_0$, the condition for synchronism in a TWT. This "force" may then synchronously excite a second harmonic wave, *both in time and space*, which makes it a much more powerful contributor to second harmonic generation. The AC harmonic current due to orbital crowding, described initially, does not possess this property of synchronization in both time and space, and is therefore a much weaker contributor in the generation of RF power at the second harmonic. However, this previous theory is able to account for the extreme case of charge overtaking, while the quasi-linear theory here cannot. Solving the governing equations in their differential form, c.f. equations (1′), (2′), and (3), also allows one to introduce non-uniform quantities in the parameters that may be due to, for example, circuit fabrication errors. This was extensively examined in [48].

Space-charge effects in TWTS

Let us now go back to the notorious problem of space-charge effects, or finding a closed form expression for Q in the Pierce picture. Many theories have been proposed that attempt to give a general formulation for calculating Q for a general beam and circuit structure. A treatise of the subtlety of this problem is given by Lau and Chernin [49], who ultimately advance the idea that Q is due to the interaction of the beam with the higher-order circuit modes (passbands higher than the fundamental). This interpretation of Q originating from residual interactions between beam and circuit, the 'remainder,' was actually also proposed by Pierce [10], who quickly abandoned such an interpretation [49], adhering instead to what the standard Pierce theory is now: the interaction between the fundamental circuit and beam modes.

Physically speaking, the calculation of the space-charge parameter boils down to calculating the 'reduced' plasma frequency ω_q of the beam. Like a plasma, the beam, which can be considered to be a non-neutral plasma, has a natural frequency called the electron beam plasma frequency, which is the frequency of the space-charge waves in an unbounded medium. However, in reality, the beam is bounded in the sense that it has a definite shape and is enclosed by the finite circuit structure. Thus, the plasma frequency of the beam is 'reduced'. In this view, the task is to calculate the reduction factor to the plasma frequency that accounts for the circuit structure (including the SWS, taking into account, for example, the 'field leakage' in the opened sections of a helix). It turns out that this calculation is intimately tied to the higher-order circuit modes mentioned in the preceding paragraph. Before we delve deeper into the mystery of space charge, it is instructive to first understand the prior art.

The most widely used approximation of the space-charge parameter QC is prescribed by Branch and Mihran [14]. In the particular case of a thin tape helix TWT with a pencil electron beam, Branch and Mihran assume that the helix is replaced with a perfectly conducting metallic cylinder of the same radius. They then calculate the plasma frequency reduction factor $F = \frac{\omega_q}{\omega_p} = \sqrt{\frac{1}{1 + (T/\beta_e)^2}}$, where the radial propagation constant T is given explicitly in terms of Bessel functions by solving Maxwell's equations in this simplified geometry. An improved model for the helix structure makes use of what is known as a sheath helix, in which current is allowed to travel

on the circuit in a helical direction [44]. But a cylinder or a sheath helix are still just approximations to the true helix structure containing geometrical complexities like the openings. Furthermore, while there are more elaborate models [44, 50] on the AC space-charge effects in a helix TWT, none give the procedure of evaluating QC. Furthermore still, these previously mentioned models are external, meaning that the determination of the space-charge parameter was done by considering a simplified version of the problem and then adding the results in ad hoc. We seek though to find a self-consistent model that takes into account the full problem (as opposed to a simplified geometry for example).

A study using the pedagogical model of a dielectric TWT that consists of a planar dielectric slab and sheet electron beam was done by Simon *et al* [51]. In that model, where an *exact* 'hot tube (including the beam)' dispersion relation may be readily derived, the idea of the higher-order circuit modes yielding Q was established conclusively. In addition, that paper showed how to accurately evaluate the Pierce parameters once a closed analytic form was found. This model however is deficient in that there is no periodic slow-wave structure in this dielectric TWT (the dielectric slows down the wave), so higher harmonics in the beam mode are excluded.

If, however, we may find an exact dispersion relation for the circuit structure including all of the geometric complexities *and* the beam dynamics for a realistic TWT, then possibly we stand a chance at determining an expression for Q. As in [49] and [51], we may cast the derived analytic dispersion relation into the form of Pierce (equations (5) or (6)) and extract an exact expression for the Pierce parameters. In [15], a formally exact treatment of the tape helix TWT without the electron beam (the 'cold-tube' dispersion relation) was presented by Chernin *et al* Later, in [52], this analysis was expanded on by the inclusion of the electron beam, giving a formally exact 'hot-tube' dispersion relation. However, because of the complexity of the analytical dispersion relation, it was unfeasible to rewrite it in a Pierce-like form. The alternative then was to numerically solve the dispersion relation and 'backtrack' to find what the Pierce parameters ought to be. In the process of doing so, it was found that it was necessary to introduce a new parameter, termed q, in order for the equations to be satisfied [39].

This new parameter q turns out to modify the circuit mode in much the same way that the original space-charge parameter Q that we were looking for modifies the beam mode, shown here for the 3-wave dispersion relation:

$$[(\beta - \beta_e)^2 - \beta_e^2 4QC^3][(\beta - \beta_{ph}) - \beta_{ph} 4qC^3] = -\beta_e^3 C^3, \tag{5'}$$

Because of this, the interpretation of q has been attributed to the effects of space charge of the beam on the circuit mode, i.e. beam loading of the circuit. This view is supported by the fact that q increases with beam current [39]. From a dispersion diagram perspective, much like how Q arises from the interaction of the fundamental beam mode with the 'remainder' of the circuit modes apart from the fundamental circuit mode, q arises from the interaction of the circuit mode with the beam modes of order higher than the fundamental, completing the symmetry. Because the dielectric TWT discussed above does NOT contain any periodic components that make up the slow-wave structure, the new parameter $q = 0$ in this model as there are no spatial harmonics of the beam [39].

To demonstrate the effects of this q term, a plot of the roots of equation (6*a*) using the standard definition of C and ubiquitous models of Q (Branch and Mihran and sheath helix [14, 44]) are given in figure 6 below along with the roots of the exact hot-tube dispersion relation for a tape helix. The three roots represent the resultant three waves from the beam-circuit interaction in the system: a neutral root, a decaying (complex with negative imaginary part) root, and an amplifying (complex with positive imaginary part) root. We, of course, care about the amplifying part as it represents the linear gain of the TWT. The other two waves however are also important as they constitute what is known as the launching loss of the TWT (where the remainder of the initial power of the signal is channeled to). Note that adding the fourth root (from solving the original 4-wave equation (5)) representing the backward propagating wave will change the results. Qualitatively, the three (main) roots will remain the same, and the fourth root will be a neutral root with a negative propagation constant.

As can be seen in figure 6, there are differences in the solution and hence the predicted gain of a helix TWT depending on the models used. From the numerical solution to the exact hot-tube dispersion relation (red in figure 6), one can find what the Pierce parameters, namely C and Q here, ought to be. These are plotted as a function of frequency below in figure 7 along with the parameters' respective models/usual definitions. The new necessary parameter q is also plotted. We see that if $q = 0$, the values of the traditional Pierce parameters take on unrealistic values, necessitating this new parameter to fit the prediction of the exact dispersion relation to Pierce theory.

One assumption of the work in [39] is that there is no cold-tube circuit loss (i.e. $Im(\Gamma_0) = 0$). There is ongoing work to extend this q-theory to consistently include the effects of attenuation [53]. Furthermore, how will the neglected backward-propagating fourth wave affect q, or the rest of the Pierce parameters for that matter? Another open question, but one under active investigation, is the analytical form of q (the casting of the exact dispersion relation into the Pierce form). This is currently being worked on, but no official literature has

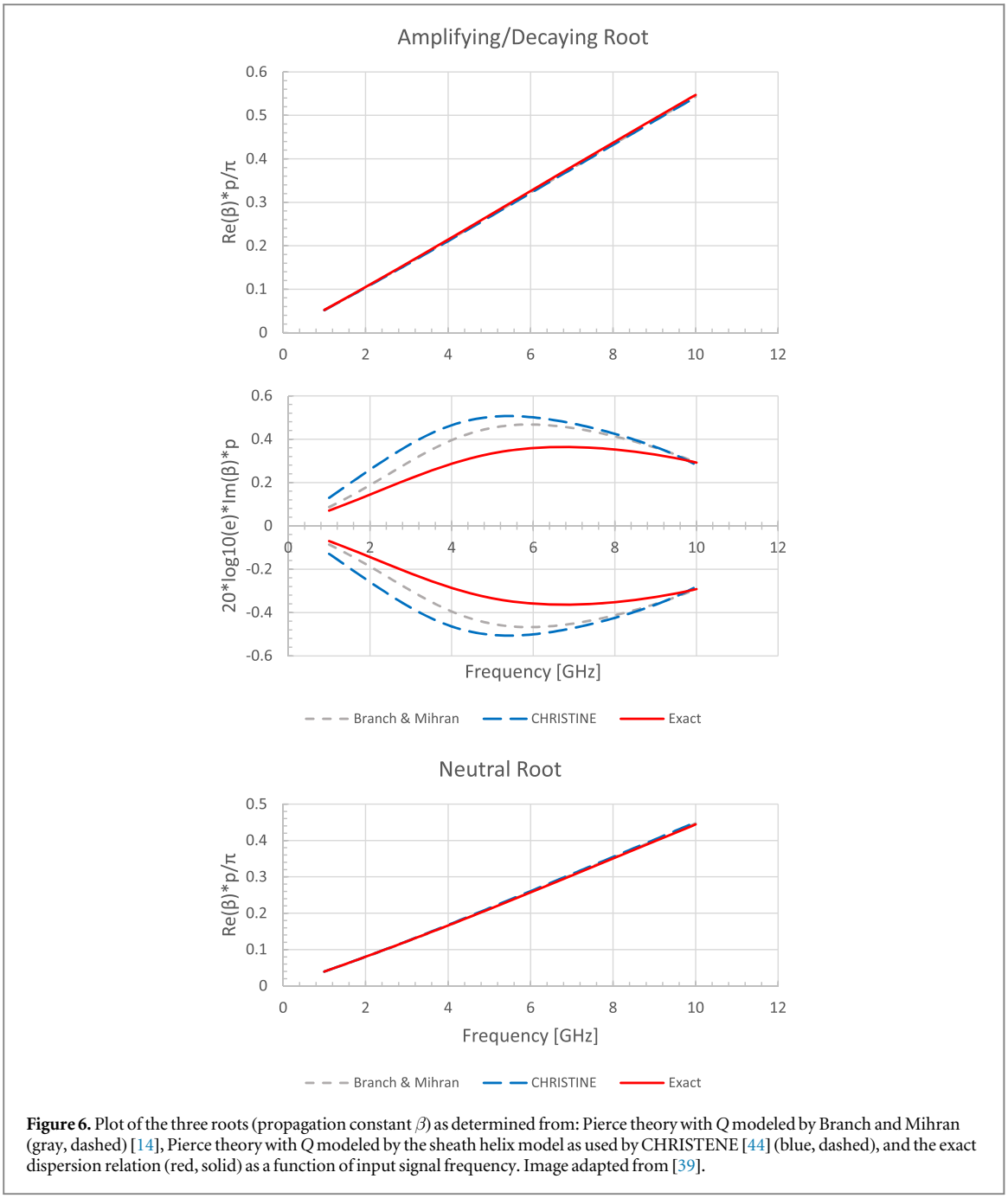

Figure 6. Plot of the three roots (propagation constant β) as determined from: Pierce theory with Q modeled by Branch and Mihran (gray, dashed) [14], Pierce theory with Q modeled by the sheath helix model as used by CHRISTENE [44] (blue, dashed), and the exact dispersion relation (red, solid) as a function of input signal frequency. Image adapted from [39].

been published yet. As a side note, a caveat of this q-theory is that even the traditionally defined Pierce parameter C is changed, due to the presence of the beam. That is, it can no longer be determined apriori. Even using the cold-tube dispersion diagram, like figure 4, proves to be a zeroth-order picture, as now not only is the beam mode changed due to space charge but the circuit mode is also perturbed. This highlights just how circular the beam-circuit interaction problem is, much like plasma physics. Thus, much remains to be done.

Discrete cavity analysis of TWTs

While the formulation thus far presented has centered around the groundwork laid by Pierce and therefore has concentrated on treating the beam-circuit interaction as a continuum, it is also important to consider 'discrete cavity' effects, relating back to the klystron-TWT picture presented in figure 1. After all, the beam-circuit interaction is not always purely continuous in a real system and having discrete effects allows for more freedom on the part of the microwave engineer to account for various effects, as will be briefly discussed below, not amenable to standard Pierce theory. This also allows us to tie the TWT to other microwave structures such as the klystron [54] and the magnetron [28], where there is not a continuous interaction.

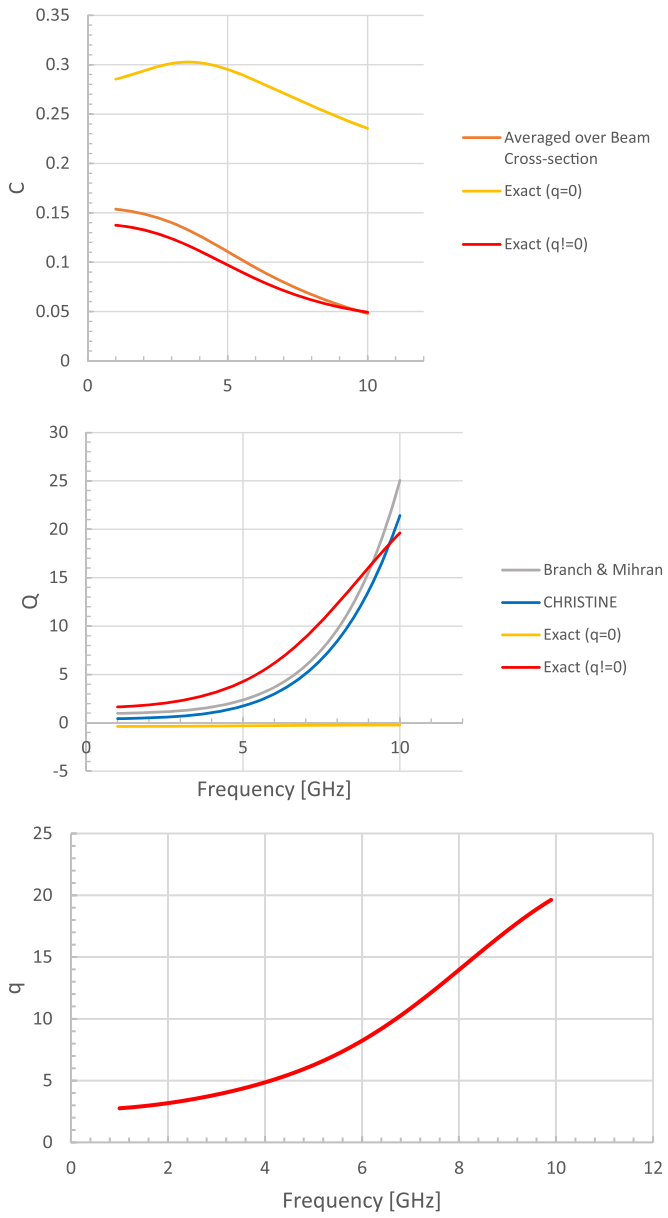

Figure 7. Plot of the Pierce parameters C and Q and new parameter q as a function of frequency of the input signal. The parameters as predicted by the exact theory (red, where $q \neq 0$) are compared to their traditional definitions: C is evaluated by averaging over the cross-section of the beam (orange) and Q is determined from Branch and Mihran (gray) [14] and the sheath helix model (blue) as used in CHRISTINE [44]. When $q = 0$, unrealistic values of the parameters are obtained (yellow). Image adapted from [39].

As we have shown, Pierce theory reduces the complex geometry of the slow wave circuit to individual traveling waves that must then interact with a driving beam. In high frequency tubes [55], as well as potential designs with relatively small numbers of cavities, the detailed adjustment of an individual cavity, either due to manufacturing errors, or for attempts to control oscillation and reflections, might be necessary. This can be challenging for Pierce theory, where we have implicitly used a wave analysis. One way to handle this is to simply allow the phase velocity mismatch, the gain parameter, and the cold-circuit loss to vary spatially in equations (6)–(9) [48]. Alternatively, another potential avenue of theoretical development comes from treating the individual cavities as discrete circuit elements with explicit coupling between the cavities. This allows individual cavities to be tuned, both in frequency and in shunt impedance, to engineer the dispersion between the beam and the electromagnetic structure, giving additional degrees of freedom to the tube designer. In terms of Pierce theory, however, the individual cavities and their coupling results in a set of normal modes. These normal modes have well-defined phase and group velocities due to the explicit nature of the coupling, just as in standard Pierce theory, but allow for non-uniform cavities to be used. Naturally, the transition from discrete normal modes to a wave formulation is well understood, as the number of cavities tends to large (infinite) values.

It should be noted that the discrete theory of TWTs has a long history. As a consequence, many developments have been made to account for various effects and ultimately advance the theory. Some more

recent examples of this are listed in [56]. There is current, on-going theoretical, simulation, and experimental work in better understanding the transition from a discrete number of cavities to an infinite continuum in a tube, from the effects that a finite number of cavities introduces to the continuous wave interaction picture of Pierce. New tube designs with a low number of cavities have been set up for this purpose of determining the limits of the Pierce theory and the transition point to the discrete cavity regime. Here, we will lay out the basics of the theoretical formulation.

For illustration purposes, we can start by considering a traveling wave structure with just four cavities. After this pedagogical introduction, we will apply the method to a real TWT. We assume a cavity can be modeled as a circuit with bulk parameters that can be well described as a harmonic oscillator. This circuit then develops a voltage due to electron beam current, source signals, and coupling between the cavities. If we define the harmonic oscillator operator L as

$$L = \left\{ \frac{d^2}{dt^2} + \frac{\omega_o}{Q}\frac{d}{dt} + \omega_o^2 \right\}, \tag{10}$$

we can then write the following set of equations for our four cavity system:

$$\begin{aligned} LA &= S + c\omega_o^2 B \\ LB &= j\omega_o^2 ZI(B) + c\omega_o^2 A + c\omega_o^2 C \\ LC &= j\omega_o^2 ZI(C) + c\omega_o^2 B + c\omega_o^2 D \\ LD &= j\omega_o^2 ZI(D) + c\omega_o^2 C, \end{aligned} \tag{11}$$

where (A, B, C, D) represent the cavity voltages, Z represents the cavity impedance, S is a general input source, c is the coupling between the cavities, and $I(x)$ represents the electron beam current at a given cavities' location. This current naturally has the impact of the previous cavities, so needs to represent a history of the current interaction with the upstream cavities. Here, we only study the cold tube properties, so we set these currents to zero, and set the source term to zero. Furthermore, take the usual actions of normalizing the resonant frequency of the isolated cavities to one without loss of generality, assuming sinusoidal solutions, and setting the quality factor to infinity, equation (11) can then be recast into matrix form,

$$\begin{aligned} &\begin{bmatrix} L & -c & 0 & 0 \\ -c & L & -c & 0 \\ 0 & -c & L & -c \\ 0 & 0 & -c & L \end{bmatrix} \begin{bmatrix} A \\ B \\ C \\ D \end{bmatrix} = \overline{\overline{M}}\,\overline{V} = 0 \\ &L = 1 - \omega^2. \end{aligned} \tag{12}$$

This equation has a number of nice features—first, it is tri-diagonal, which allows considerable linear algebra tools to be used. Second, all of the cavity details can be included in the matrix **M**. Thus, equation (12) gives us the homogenous solution to our slow wave structure. Sources can be added to the right hand side of equation (12) as we go forward.

Here, however, we will continue to focus on the eigenvalues of this system. These eigenvalues give the resonant frequencies of the system and the eigenvectors are the characteristic modes. Analytically, we can exploit the fact that tri-diagonal systems have a recursion relationship for the determinant. Furthermore, we use the fact that we have only four cavities and thus have a quartic equation, which is actual bi-quadratic. Alternatively, we can use Octave's symbolic package to solve for the roots of the system, or numerically solve for them. Because the resulting equations are polynomial in nature, the numerical solution with Octave is quite tedious, even for four cavities. Once a given root is found, the equations need to be deflated by hand for Octave's numerical solver to find the next root [57]. Despite this challenge, analytic, symbolic and numerical all gave the same resonant frequencies for our four cavity system:

$$\begin{aligned} \omega_1 &= \sqrt{1 - 1.62c} \\ \omega_2 &= \sqrt{1 + 1.62c} \\ \omega_3 &= \sqrt{1 - 0.62c} \\ \omega_4 &= \sqrt{1 + 0.62c}, \end{aligned} \tag{13}$$

where we note, for clarity, that 'c' is the coupling between adjacent cavities.

We can then use equation (13) to solve for the eigenvectors of the system. The plot of these is shown in figure 8. Initially, these eigenvectors were difficult to interpret, but noting that these are normal modes, the shape of these fields makes more sense. To do this, we need to fix the boundary conditions outside of the cavity structure—a typical choice is to set the fields to zero, which would be consistent with a TWT slow wave structure inside a cutoff waveguide. With these conditions, the normal modes become the typical phase advance per cavity if one assumes an additional 'virtual cavity' with amplitude of zero on either side of the slow wave structure. This

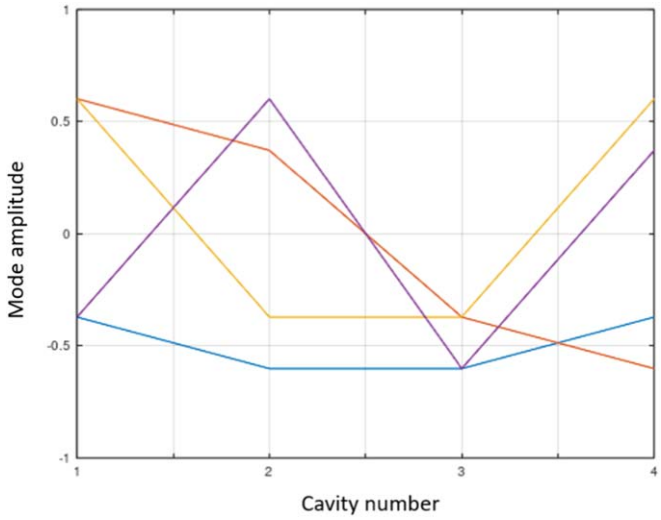

Figure 8. Eigenvectors for the four cavity system roots given in equation (13) from Octave. This plots mode amplitude versus cavity number. Thus, the horizontal axis gives the axial location of the field.

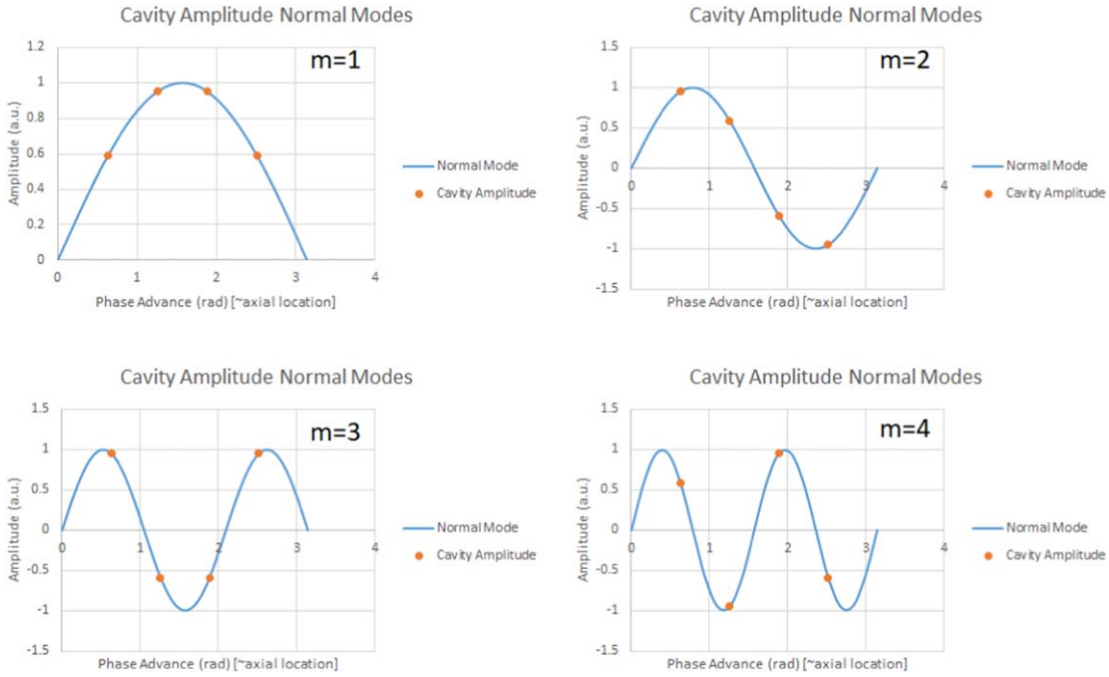

Figure 9. Analytic normal mode analysis of the 4 cavity eigenvectors.

is shown in figure 9. Comparing figures 8 and 9, we see that the orange points in the plot, representing the cavity field amplitude, are following a given sinusoidal pattern, albeit with a difference in phase for two of the eigenvectors between the Octave result and our normal model analysis. These modes can be directly tied to the phase advance per cavity, which is given by $m\pi/4$, where m is an integer. With this insight, it is possible to plot the dispersion relationship for our model with frequency versus phase advance (or mode number) as shown in figure 10.

It is worth noting that figure 10 has the typical characteristics of dispersion relationships that we expect from relatively short slow wave structures. The correct phase advance and mode shape have been found. Additionally, variation in the number of cavities and/or the cavity coupling allows the relative 'flatness' of the curve near the π mode to be observed, consistent with experimental and frequency domain analysis of TWT structures. Finally, it is a positive sign that we have tested the computational tools that are necessary to handle realistic numbers of cavities for a non-trivial if small, example, and verified these tools against analytic results.

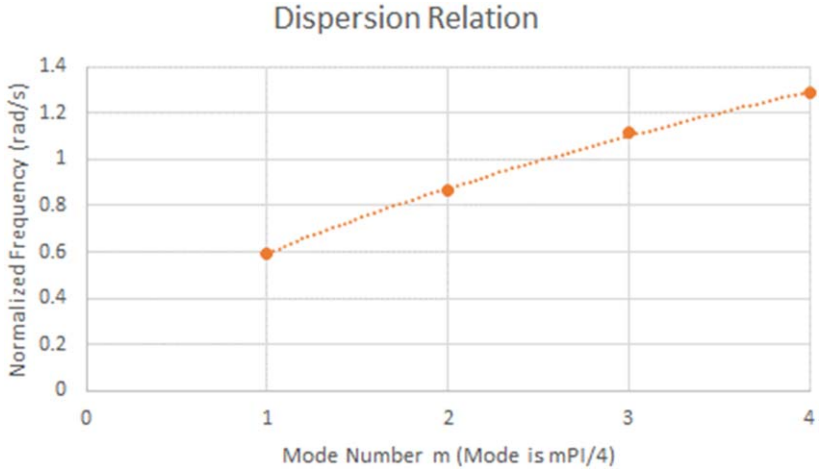

Figure 10. Dispersion relation for our four cavity circuit model. Cavity coupling $c = 0.4$.

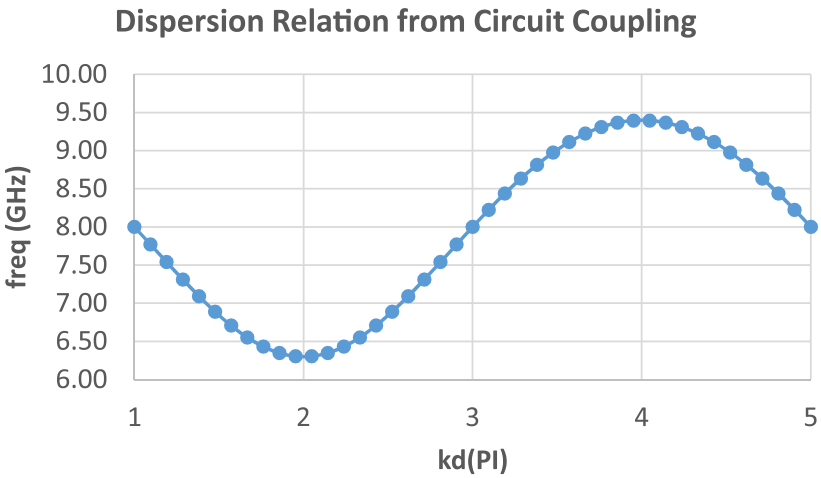

Figure 11. Dispersion relation for a 20 cavity sine waveguide TWT constructed from a coupled cavity approach. Individual cavities have a resonant frequency of 8 GHz and the dimensionless coupling between the cavities is $c = 0.19$.

Next, we extend the coupled-cavity circuit model to simulate a realistic TWT [e.g. using the parameters from [55]], as opposed to the four-cavity proof-of-principle. The effort proceeds by building a tridiagonal matrix with the harmonic oscillator operator on the diagonal and the coupling term on the bands. For our exercise here, we assume no ohmic loss and symmetric coupling between the cavities. In this case, we have a Toeplitz matrix, and there are recursion relations for the eigenvalues. This allows us to compute the dispersion relationship from the normal modes. Because the harmonic oscillator operation has two roots, there are two harmonic oscillator modes for the dispersion relation. The dispersion relation is shown in figure 11. This result is in excellent agreement with HFSS results published in the literature [55].

The next passband is found in a similar manner, with the resonant frequency of an individual cavity changed to 12.5 GHz and the coupling reduced to $c = 0.03$. The physical reason for the reduction in the cavity coupling for the second passband is the higher frequency allows the electromagnetic waves to be concentrated more tightly to the structure. It is also worth noting that both passbands have significantly more coupling than the klystron cases previously examined. This is simply the nature of the traveling wave tube structure. The second passband is shown in figure 12.

Comparing the coupled circuit model and HFSS does unveil an interesting feature. Simply taking one harmonic oscillator mode (or 'branch cut' as it is referred to in figure 12) of the normal mode structure yields the orange curve in figure 12. This is clearly different than that seen in the HFSS calculation. However, switching to the other harmonic oscillator mode allows us to find the correct dispersion relationship for both modes in the second passband. The jump between harmonic oscillator modes is not clear, and further work needs to be done

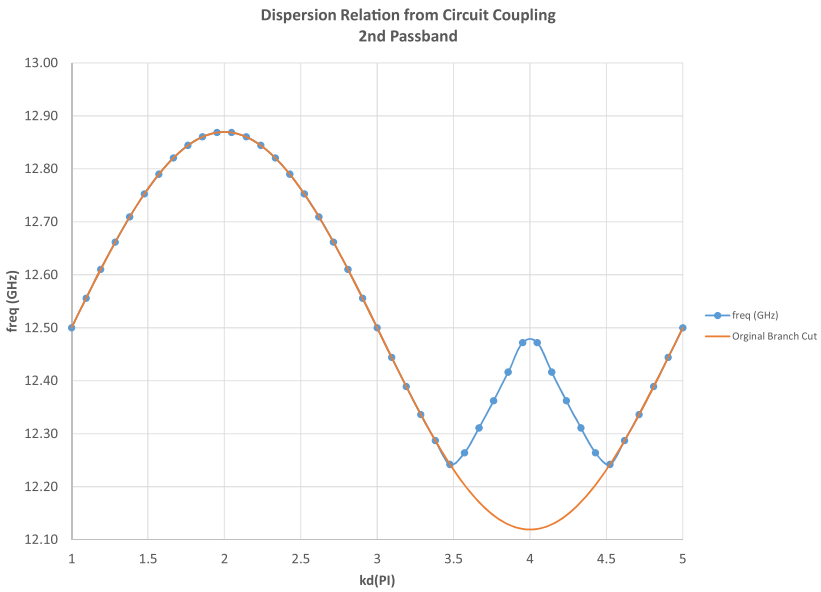

Figure 12. Second passband for the sine waveguide TWT with individual cavity frequency of 12.5 GHz and cavity coupling of $c = 0.03$.

to understand why this additional step is necessary to reproduce the second passband. That said, we believe this kink is physical, and structures like these are often found in band edges of TWTs. Additionally, the HFSS calculations were run on a unit cell, and it is not clear if that makes it easier to choose between the harmonic oscillator modes [58].

We have demonstrated that a coupled circuit model can reproduce the electromagnetic structure of a full TWT, and that this allows one to add spatial non-uniformity to the slow wave circuit. Additional work that we have done shows that as the number of cavities becomes large, the normal mode analysis naturally transitions to a wave description. This provides an explicit link between standard Pierce theory (wave) and a means to incorporate finite length effects, internal reflections, manufacturing errors, and individual cavity differences into a Pierce style analysis.

Concluding remarks

In conclusion, we have just glossed over the mode-coupling theory of Pierce in describing the beam-circuit interaction of a TWT. We have talked qualitatively and quantitatively about the linear DC electron beam and the electromagnetic signal on the surrounding structure constituting the circuit, separately, and then how both interact to produce the desired amplification of the signal. Even though Pierce's classical theory is a linear (so-called 'small-signal') theory, it is still powerful and widely used. The key to its endurance is its simplicity as well as tradition, as it was the first comprehensive theory to describe the inner workings of a TWT. Its simplicity allows for relatively fast 'back-of-the-envelope' calculations and insights into the underlying mechanisms of beam-circuit interaction. Here, we stress what we believe are the core ideas of Pierce's theory: synchronous interaction between and coupling of the beam and circuit producing amplification of the input signal.

In keeping with this, we attempt to provide several natural extensions to the Pierce theory to describe phenomena not previously considered in the small-signal regime. These include harmonic generation (from dynamical synchronous interaction between the beam and circuit in an octave bandwidth tube) and beam-loading on the circuit (stressing the symmetry between beam and circuit and their coupling). Additionally, we have discussed the links between normal mode analysis associated with coupling individual cavities and its relationship to Pierce theory.

It should be stressed that this paper is by no means a comprehensive overview of TWTs. This paper is much too immature to tackle such a subject. We wish to introduce the reader to the world of TWTs and beam-circuit interactions via the classical theory of Pierce and try to extend the core ideas behind the theory to tackle more modern topics: harmonic generation, space-charge effects, and discrete cavity effects. There are still many topics

to explore. The reader is encouraged to look through the references (which is by no means extensive), especially [59] on the history of the TWT in telecommunication. Louisell's textbook [60] provides excellent, more in-depth discussions on many of the topics addressed here, especially space-charge waves (c.f. Chapters 2 and 3).

Acknowledgments

This work was supported by the Air Force Office of Scientific Research (AFOSR) Multidisciplinary University Research Initiative (MURI) Grant No. FA9550-18-1-0062, Air Force Office of Scientific Research (AFOSR) YIP Grant No. FA9550-18-1-0061, and the Office of Naval Research (ONR) YIP Grant No. N00014-20-1-2681.

The authors would also like to thank Professor Y. Y. Lau for valuable discussions and his advice and encouragement.

ORCID iDs

Patrick Wong https://orcid.org/0000-0002-8437-6990
Peng Zhang https://orcid.org/0000-0003-0606-6855
John Luginsland https://orcid.org/0000-0002-6130-6156

References

[1] Gilmour A S Jr. 1994 *Principles of Traveling Wave Tubes* 2nd edn (Norwood, MA, USA: Artech House)
[2] Gilmour A S Jr. 2011 *Klystrons, Traveling Wave Tubes, Magnetrons, Crossed-Field Amplifiers, and Gyrotrons* 1st edn (Norwood, MA, USA: Artech House)
[3] Gewartowski G W and Watson H A 1966 *Principles of Electron Tubes* (Princeton, NJ, USA: Van Nostrand)
[4] Tsimring S E 2007 *Electron Beams and Microwave Vacuum Electronics* (Hoboken, NJ, USA: John Wiley & Sons, Inc)
[5] Kompfner R 1964 *The Invention of Traveling Wave Tube* (San Francisco, CA: San Francisco Press)
[6] Lindenblad N E 1942 Electron discharge device system *U.S. Patent* 2300052
[7] Haeff A V 1941 1936 Device for and method of controlling high frequency currents *U.S. Patent* 2064469 and 2233126
[8] Edward E, David Jr, Max V, Mathews A and Noll M 1910–2002 *A biographical memoir* (Washington, D.C: The National Academies Press)
[9] The traveling-wave tube image is public domain (originally from: Franklin Loomis 1953 Bell system plans for broadband network facilities *Tele-Tech* (Bristol, Connecticut: Magazine, Caldwell-Clements Inc.) Vol 12, p 80 fig. 6 on American Radio History)
[10] Pierce J R 1950 *Traveling Wave Tubes* (New York, NY, USA: Van Nostrand)
[11] Field L M 1949 Some slow-wave structures for traveling-wave tubes *Proc. IRE* **37** 34–40
Levush B, Abe D, Pasour J, Cooke S, Wood F, Larsen P, Nguyen K, Wright E, Pershing D and Balkcum A 2013 Sheet electron beam millimeter-wave amplifiers at the Naval Research Laboratory *IEEE Int. Conf. on Microwaves, Communications, Antennas and Electronic Systems (COMCAS 2013)* (https://doi.org/10.1109/COMCAS.2013.6685231)
[12] Tan Y S and Seviour R 2009 Wave energy amplification in a metamaterial-based traveling-wave structure *EPL* **87** 34005
[13] Yurt S C, Elfrgani A, Fuks M I, Ilyenko K and Schamiloglu E 2016 Similarity of properties of metamaterial slow-wave structures and metallic periodic structures *IEEE Trans. Plasma Sci.* **44** 1280–6
[14] Branch G M and Mihran T G 1955 Plasma frequency reduction factors in electron beams *IRE Trans.—Electron Devices* **2** 3–11
See also: Ramo S 1939 The electronic-wave theory of velocity-modulation tubes *Proc. of the I.R.E.* **27** 757–63
[15] Chernin D, Antonsen T M Jr. and Levush B 1999 Exact treatment of the dispersion and beam interaction impedance of a thin tape helix surrounded by a radially stratified dielectric *IEEE Trans. Electron Devices* **46** 1472–83
[16] Johnson H R 1955 Backward-wave oscillators *Proc. IRE* **43** 684–97
[17] Kuznetsov A P, Kuznetsov S P, Rozhnev A G, Blokhina E V and Bulgakova L V 2004 Wave theory of a traveling-wave tube operated near the cutoff *Radiophys. Quantum Electron.* **47** 356–73
[18] Hung D M H, Rittersdorf I M, Zhang P, Chernin D, Lau Y Y, Antonsen T M Jr., Luginsland J W, Simon D H and Gilgenbach R M 2015 Absolute instability near the band edge of traveling-wave amplifiers *Phys. Rev. Letters* **115** 124801
[19] Antoulinakis F, Wong P, Jassem A and Lau Y Y 2018 Absolute instability and transient growth near the band edges of a traveling wave tube *Phys. Plasmas* **25** 072102
[20] Shockley W 1938 Currents to conductors induced by a moving point charge *J. A. P.* **9** 635
Ramo S 1939 Currents induced by electron motion *Proc. I.R.E.* **27** 584–5
[21] Abrams R H, Levush B, Mondelli A A and Parker R K 2001 Vacuum electronics for the 21st century *IEEE Microwave Mag.* **2** 61–72
[22] Huang Z and Kim K J 2007 Review of x-ray free electron laser theory *Phys. Rev. Special Topics—Accelerator and Beams* **10** 034801
Roberson C W and Sprangle P 1989 A review of free-electron lasers *Phys. Fluids* B **1** 3
Marshall T C 1985 *Free Electron Lasers* Macmillan) 1st edn
Freund H P and Antonsen T M 1996 *Principles of Free-electron Lasers* 2nd edn (US: Springer)
[23] Kumar V and Kim K J 2006 Analysis of Smith-Purcell free-electron lasers *Phys. Rev.* E **73** 026501
[24] Schachter L 2011 *Beam-wave Interaction in Periodic and Quasi-periodic Structures* 2nd edn (Berlin, Germany: Springer)
[25] Zhang P, Ang L K and Gover A 2015 Enhancement of coherent Smith-Purcell radiation at terahertz frequency by optimized grating, prebunched beams, and open cavity *Phys. Rev. Special Topics—Accelerators and Beams* **18** 020702

[26] Granatstein V L and Alexeff I 1987 *High Power Microwave Sources* (Boston: Artech House)
[27] Chu K R 2004 The electron cyclotron maser *Rev. Mod. Phys.* **76** 489–540
[28] Barker R J, Booske J H, Luhmann N C and Nusinovich G S 2005 *Modern Microwave and Millimeter-wave Power Electronics* (Piscataway, New Jersey: IEEE Press)
[29] Benford J, Swegle J A and Schamiloglu E 2016 *High-power microwaves* 3rd edn (New York: CRC Press)
[30] Thumm M 2016 *State-of-the-art of High Power Gyro-devices and Free Electron Masers* KIT Scientific Publishing)
Nusinovich G S 2004 *Introduction to the Physics of Gyrotrons* (Baltimore: Johns Hopkins University Press)
[31] Shiffler D, Luginsland J, French D M and Watrous J 2010 A cerenkov-like maser based on a metamaterial structure *IEEE Trans. Plasma Sci.* **38** 1462–5
[32] Hoff B W and French D M 2016 Simulations of a disk-on-rod TWT driven by an NLTL-modulated electron beam *IEEE Trans Plasma Sci.* **44** 1265–9
Zhang P, Hoff B, Lau Y Y, French D M and Luginsland J W 2012 Excitation of a slow wave structure *Phys. Plasmas* **19** 123104
[33] Pierce J R 1954 Coupling of modes of propagation *J. Appl. Phys.* **25** 179
[34] Haus H A and Huang W P 1991 Coupled-mode theory *Proc. IEEE* **79** 1505–18
[35] Birdsall C K and Brewer G R 1954 Traveling wave tube characteristics for finite values of C *IRE Trans. PGED* **ED-1** 1–11
[36] Antonsen T M Jr., Safier P, Chernin D P and Levush B 2002 Stability of traveling-wave amplifiers with reflections *IEEE Trans. Plasma Science* **30** 1089–107
[37] Chernin D, Rittersdorf I, Lau Y Y, Antonsen T M Jr. and Levush B 2012 Effects of multiple internal reflections on the small-signal gain and phase of a TWT *IEEE Trans. Electron Devices* **59** 1542–50
[38] Booske J H and Converse M C 2004 Insights from one-dimensional linearized pierce theory about wideband traveling-wave tubes with high space charge *IEEE Trans. Plasma Science* **32** 1066–72
[39] Wong P Y, Chernin D and Lau Y Y 2018 Modification of pierce's classical theory of traveling-wave tubes *IEEE Electron Device Lett.* **39** 1238–41
[40] Nordsieck A 1953 Theory of the large signal behavior of traveling-wave amplifiers *Proceedings of the I.R.E.* **41** 630–7
[41] Tien P K, Walker L R and Wolontis V M 1955 A large signal theory of traveling-wave amplifiers *Proc. of the I.R.E.* **43** 260–77
Rowe J E 1956 A large-signal analysis of the traveling-wave amplifier: theory and general results *IRE Trans.—Electron Devices* **3** 39–56
Giarola A J 1968 A theoretical description for the multiple-signal operation of a TWT *IEEE Trans. Electron Devices* **ED-15** 381–95
Dionne N J 1970 Harmonic generation in octave bandwidth traveling-wave tubes *IEEE Trans. Electron Devices* **ED-17** 365–72
[42] Wilsen C B, Lau Y Y, Chernin D P and Gilgenbach R M 2002 A note on current modulation from nonlinear electron orbits *IEEE Trans. Plasma Science* **30** 1176–8
Lau Y Y, Chernin D P, Wilsen C and Gilgenbach R M 2000 Theory of Intermodulation in a Klystron *IEEE Trans. Plasma Science* **28** 959–70
[43] Dong C F, Zhang P, Chernin D, Lau Y Y, Hoff B W, Simon D H, Wong P, Greening G B and Gilgenbach R M 2015 Harmonic content in the beam current in a traveling-wave tube *IEEE Trans. Electron Devices* **62** 4285–92
[44] Antonsen T M Jr. and Levush B 1998 Traveling-wave tube devices with nonlinear dielectric elements *IEEE Trans. Plasma Sci.* **26** 774–86
[45] Wong P Y, Lau Y Y, Chernin D, Hoff B W and Gilgenbach R M 2018 Origin of second-harmonic signals in octave bandwidth traveling-wave tubes *IEEE Trans. Electron Devices* **65** 710–5
[46] Datta S K, Jain P K, Raj Narayan M D and Basu B N 1998 Nonlinear eulerian hydrodynamical analysis of helix traveling-wave tubes *IEEE Trans. Electron Devices* **45** 2055–62
[47] Nicholson D R 1983 *Introduction to Plasma Theory* p 31(New York: Wiley)
[48] Rittersdorf I M, Antonsen T M Jr., Chernin D and Lau Y Y 2013 Effects of random circuit fabrication errors on the mean and standard deviation of small signal gain and phase of a traveling wave tube *IEEE J. Electron Device Soc.* **1** 117–28
Pengvanich P, Chernin D, Lau Y Y, Luginsland J W and Gilgenbach R M 2008 Effect of random circuit fabrication errors on small-signal gain and phase in traveling-wave tubes *IEEE Trans. Electron Devices* **55** 916–24
[49] Lau Y Y and Chernin D 1992 A review of the ac space charge effect in electron-circuit interactions *Phys. Fluids* B **4** 3473–97
[50] Cooke S J, Chang C-L, Antonsen T M Jr., Chernin D P and Levush B 2005 Three-dimensional modeling of AC space charge for large signal TWT simulation *IEEE Trans. Electron. Devices* **52** 764–73
Dialetis D, Chernin D, Antonsen T M Jr. and Levush B 2007 An Improved Representation of AC space-charge fields in steady-state simulation codes for linear-beam tubes *IEEE Trans. Electron Devices* **54** 888–92
Datta S K and Kumar L 2009 A simple closed-form formula for plasma-frequency reduction factor for a solid cylindrical electron beam *IEEE Trans. Electron Devices* **56** 1344–6
[51] Simon D H, Wong P, Chernin D, Lau Y Y, Hoff B, Zhang P, Dong C F and Gilgenbach R M 2017 On the evaluation of Pierce parameters C and Q in a traveling wave tube *Phys. Plasmas* **24** 033114
[52] Wong P Y 2018 A contemporary study in the theory of traveling-wave tubes *Ph. D. Dissertation* Univ. Michigan
[53] Jassem A, Lau Y Y, Chernin D P and Wong P 2020 Theory of traveling wave tube including space charge effects on the circuit mode and distributed cold tube loss *PUBLISHED in IEEE Trans. Plasma Sci.* (https://doi.org/10.1109/TPS.2020.2969049)
[54] Luginsland J W, Lau Y Y, Hendricks K J and Coleman P D 1996 A model of injection-locked relativistic klystron oscillator *IEEE Trans. Plasma Sci.* **24** 935–7
[55] Hoff B W, Simon D S, French D M, Lau Y Y and Wong P 2016 Study of a high power sine waveguide traveling wave tube amplifier centered at 8 GHz *Phys. Plasmas* **23** 103102
[56] Minenna D F G, Terentyuk A G, André F, Elskens Y and Ryskin N M 2019 Recent discrete model for small-signal analysis of traveling-wave tubes *Phys. Scr.* **94** 055601
Minenna D F G, Elskens Y, André F, Poyé A, Puech J and Doveil F 2019 DIMOHA: a time-domain algorithm for traveling-wave tube simulations *IEEE Trans. Electron Devices* **66** 4042–7
André F, Bernardi P, Ryskin N M, Doveil F and Elskens Y 2013 Hamiltonian description of self-consistent wave-particle dynamics in a periodic structure *EPL* **103** 28004
[57] Press W H, Teukolsky S A, Vetterling W T and Flannery B P 2007 *Numerical Recipes 3rd edition: The Art of Scientific Computing* (Cambridge: Cambridge University Press)
[58] Simon D 2019 private communication
[59] Minenna D, André F, Elskens Y, Auboin J-F, Doveil F, Puech J and Duverdier É 2018 'The Traveling-Wave Tube in the History of Telecommunication,' HAL archives: hal-01754885 (https://doi.org/10.1140/epjh/e2018-90023-1)
[60] Louisell W H 1960 *Coupled Mode and Parametric Electronics* (New York and London: J. Wiley and Sons)